Excitation of the L Intermediate of Bacteriorhodopsin: Electric Responses to Test X-Ray Structures

R. Tóth-Boconádi,* A. Dér,* S. G. Taneva,† and L. Keszthelyi*
*Institute of Biophysics, Biological Research Centre, Hungarian Academy of Sciences, Szeged, Hungary; and †Institute of Biophysics, Bulgarian Academy of Sciences, Sofia, Bulgaria

ABSTRACT The L intermediate of bacteriorhodopsin was excited, and its electrical response was measured. Two positive components were found in it with respect to the direction of proton pumping: an unresolved fast component, and a slower one ($\tau = 7$ μs) of small amplitude. The fast component was assigned to a charge motion corresponding to reisomerization of the retinal moiety, whereas the slow one was attributed to charge rearrangements reestablishing the ground state. Because three x-ray crystallographic structures have recently been reported for the L intermediate, it seemed important to calculate the intramolecular dipole moment changes associated to bR→L for all three structures, so as to compare them with similar quantities determined from the electrical signals. The results are discussed in terms of amino acid side chains possibly contributing to the observed effect. We propose to use electrical signals as a verification tool for intermediate structures of the photocycle, and thus for molecular models of proton pumping.

INTRODUCTION

Bacteriorhodopsin (bR), a paradigm for ion pumps and the 7-helix receptor family, is expected to be the first ion transporting membrane protein whose function can be described on the level of atoms, purely by physical methods (1–4). Recent determination of x-ray structures (5) clearly represents an important step in this direction, and inspired mechanistic models of proton pumping (6–8). The question arises, however, whether the currently available x-ray structures, determined under far-from-natural conditions, represent a solid basis on which one can build functional models reflecting the complex dynamical behavior of a protein in action at room temperature.

In this article, we address this problem via analyzing the x-ray data available for the L intermediate structure in terms of their compatibility with photoelectric signals associated to L. For the time being, most of the x-ray data are piled up in connection with this intermediate (9–12). At the first sight, they look somewhat different from each other, which has been attributed to methodological differences in sample preparation and mainly in interpretation of the raw data (13).

Since even these small differences might give rise to establish fundamentally different models of proton pumping (13), it is important to find reliable experimental verification tools that are able to select among different x-ray structures. In a previous article (14), we suggested photoelectric signals of bR (protein electric response signals (PERS)) (15) to use as such a reference tool. From the kinetic traces, electric dipole moment changes between photocycle intermediates can be determined, which can be directly compared with similar quantities calculated from structural data.

Here we report on a study comparing the direction and size of the charge displacement between the bR ground state and the L intermediate, determined experimentally from photoelectric measurements, and calculated from different x-ray structures available in the literature.

First we present electric signals corresponding to excitation of the L intermediate, and establish that, similar to K and M (16–22), and unlike N and O (23–25), the photoreaction of the L form also results in a charge displacement opposite to that of the overall pumping direction, corresponding to a shortcut of the photocycle redirected from L to the ground state.

In the next step we determine the sign of the electric dipole moment change between bR and L, and compare it with the same quantity derived from three different pairs of x-ray structures. General implications of the results are discussed.

MATERIALS AND METHODS

Purple membrane containing wild-type bR was separated from *Halobacterium salinarum* strain R_1M_1. The membrane fragments were oriented and immobilized in polyacrylamide gel as described in Dér et al. (26). Slabs measuring $1.6 \times 1.6 \times 0.18$ cm^3 were cut and soaked in a solution (100 cm^3 containing 50 μM $CaCl_2$ at pH 7.5) for overnight at least, and placed, in the same solution, into cuvettes.

Two lasers were used for flash illumination: a frequency-doubled Nd:YAG laser (530 nm) (Surelite, Continuum, Santa Clara, CA) and an excimer laser-driven dye laser with fluorescein 27 (553 nm) (Lambda Physik, Göttingen, Germany). The Nd:YAG laser provided the first flash and the dye laser the second. A laboratory-built time generator controlled the delay between the flashes.

The electric responses were picked up with platinized Pt electrodes immersed in the solution and amplified by a homemade current amplifier based on a Burr-Brown 3554 operational amplifier with band width set to

Submitted June 15, 2005, and accepted for publication December 22, 2005.

Address reprint requests to A. Dér, Institute of Biophysics, Biological Research Centre, Hungarian Academy of Sciences, Szeged, PO Box 521, Hungary 1113. Tel.: 36-62-599607; Fax: 36-62-433133; E-mail: derandra@nucleus.szbk.u-szeged.hu.

0006-3495/06/04/2651/05 $2.00

doi: 10.1529/biophysj.105.068817

300 kHz. The signals were digitized and averaged by computer-controlled transient recorder (Lecroy, Santa Clara, CA) with 10,000 channels.

For the charge displacement/dipole moment calculations, the atomic coordinates of the bR and L structures were taken from the published PDB files (1E0P, 1O0A, and 1UCQ) (9–11), whereas the corresponding partial charge values were adapted from earlier molecular dynamics simulations. Partial charge data sets are provided in Supplementary Materials. For details of their assay, see Humphrey et al. (27) and McKerell et al. (28). H atoms were added to the structures by the molecule modeling software HyperChem 3 (Autodesk, San Rafael, CA). The calculations were restricted to amino acids Arg-82, Asp-85, Leu-93, Trp-182, Asp-212, and Lys-216, and the retinal moiety; water molecules and temperature factors were not taken into account. The quantity $\mu^z_{bR-L} = \sum(z(i)_L - z(i)_{bR})q(i)$ was determined for all the intermediate structures, where $z(i)$ is the z coordinate of the ith atom, $q(i)$ the corresponding partial charge, and summation runs through all the atoms considered.

RESULTS AND DISCUSSION

The L intermediate was generated by a flash exciting the ground state (bR), and then it was subjected to a second flash to investigate its photoresponse. The major problem in studying PERS of a given intermediate is the separation of its contribution from signals due to the unavoidable excitation of the residual ground state (bR) and other intermediates generated by the first flash (residual means the fraction not excited by the first flash.) The population of these species changes with the intensity of the first and the delay time of the second flash. The ideal separation can only be approximated. In this special case, we assumed that at the wavelength of the second flash (553 nm) only the L intermediate and the residual ground state were excited. Three excitation measurements were performed: by the first flash only (Fig. 1, trace *a*), by both flashes (trace *b*, at different delay times between them), and by the second flash (trace *c*). Traces *a* and *c* show the well known PERS of bR in the given time range: a large fast negative signal followed by positive components (29). In a simplified explanation, the negative signal is assigned to the bR-K-L transitions, whereas the first positive signal follows the L decay. At trace *b*, the sum of the responses for excitation of bR, the residual ground state (i.e., a part *P* of the signal in trace *c*), and the intermediate appear at the given delays (4 μs in Fig. 1). In Fig. 1, the fast signal at 4 μs delay is smaller in trace *b* than in trace *c*, meaning a positive contribution from the L intermediate, confirming a previous result (19).

Accurate determination of factor *P* is necessary to obtain information on other possible components in addition to the fast responses. Therefore, we recorded PERS generated by a double flash in a delay range where the concentration of the other intermediates was negligible. Subtracting these values at different delays, the remaining signals are attributed to the L intermediate. If the procedure is correct, then the amplitudes of the fast signals follow the L decay.

The delay-time dependence of the amplitude of the fast signals, recorded after the second flash in double excitation, is shown in Fig. 2. The negative amplitude increases according to the lifetime of L decay, then levels off for a first plateau, and increases again to a second plateau with the lifetime of the rate-limiting step of the photocycle. The ratio of the first and second plateau values is $P = 0.65$. The difference between traces $(b - a) - P \times c$ is assigned to the PERS of the excited L intermediate. In Fig. 3, the positive amplitudes of the fast signals calculated this way are normalized to the electric signal assigned to L decay. Their close agreement substantiates the outlined procedure. According to Fig. 4, the L PERS consists of a large, fast positive signal and another positive signal of 7.3 $\pm$ 0.1 μs lifetime with smaller amplitude. The ratio of the areas of the slow and fast signals is 0.061 $\pm$ 0.001. The integral of line *a* for the whole photocycle and, similarly, the integral of $b - P \times c$, is proportional to the transported charge. The second is smaller with 18%, indicating that excitation of L stops the charge

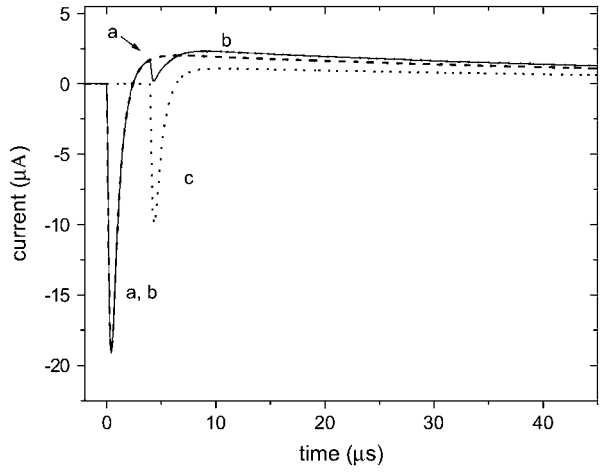

FIGURE 1 Traces of electric responses in the case of the L intermediate: (*a*) only the first flash (530 nm); (*b*) double flash (the second flash, 553 nm, at a 4-μs delay); and (*c*) only the second flash. Solution: 50 μM $CaCl_2$, pH 7.5, at 24°C.

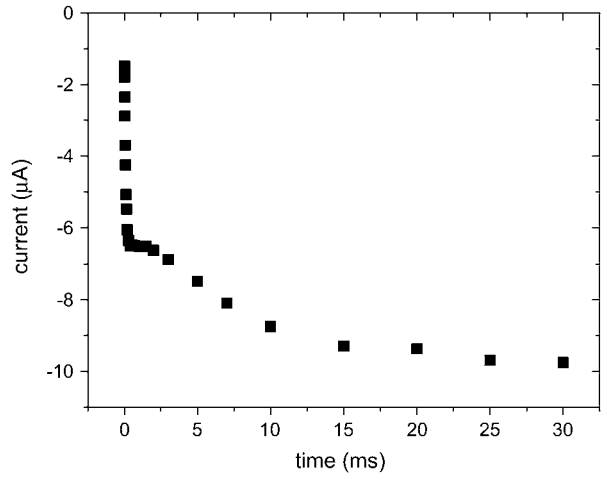

FIGURE 2 Delay-time dependence of the amplitudes of the fast current signal excited by the second flash in the case of the L intermediate.

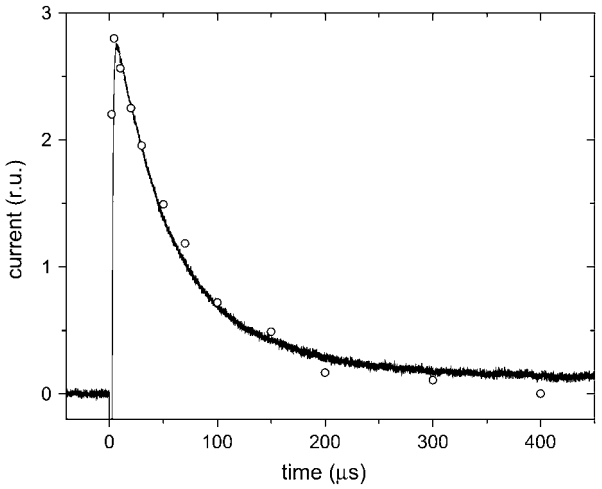

FIGURE 3 Derived amplitudes (see text) from the fast-current signal for L excitation (○) normalized to the electric signal (*solid line*) assigned to L decay.

transport, i.e., shortcuts the photocycle with ~50% quantum efficiency.

When interpreting the electric signals measured upon excitation of L, it is worth recalling what is known about the opposite process. PERS of ground state bR until L has two negative components: the lifetime of the first is between 2.5 and 5 ps (22), whereas that of the second is $\approx 2\ \mu$s (29). The first was assigned to charge motions during the bR → K, and the second to that during the K → L transition (15). They were attributed to primary charge separation upon light excitation inducing all *trans* to 13-*cis* isomerization, and to some unknown charge rearrangement during the K → L transition.

Taking these facts into account, the unresolved positive fast signal of L obviously represents the charge motion corresponding to reisomerization of the retinal from 13-*cis* to all-*trans*, whereas the small positive component of L must represent a charge motion accompanying the conformational

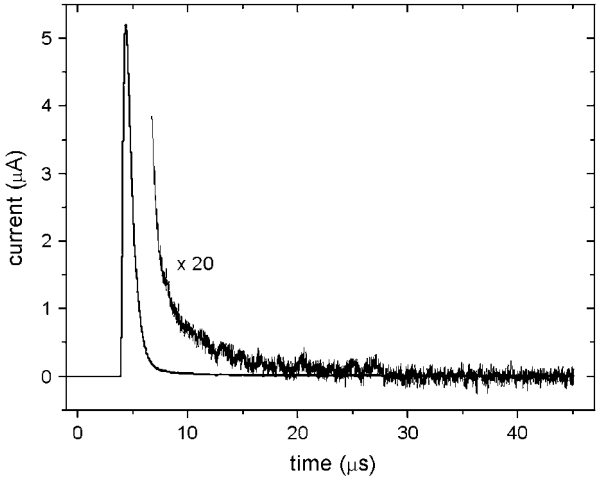

FIGURE 4 Electric response for excitation of the L intermediate.

rearrangement reestablishing bR. The question arises whether all these are commensurate with the x-ray structures published so far, and, if yes, what kind of charge rearrangements in the protein molecule contribute the most to the measured electric signal.

Crystallographic structures of K and L intermediates have already been determined, though L structures from different groups (1E0P, 1O0A, 1UCQ) deviate somewhat from each other (9–12). A careful comparison of the three reported L structures is given by Lanyi (13). Although none of the three models were found to be free from some degree of conflict, an overall preference was given to 1O0A, on the basis of mainly methodological considerations. In general, it was concluded that low-temperature structures are probably relevant to proton pumping of bR at ambient temperature.

Comparison of the published x-ray structures of the three research groups agree in the finding that, besides retinal, only a few amino acids are affected during the bR → L (or L → bR) transition. Following Lanyi (13), we considered six amino acids (Arg-82, Asp-85, Leu-93, Trp-182, Asp-212, and Lys-216) and the retinal moiety as the main contributors to the charge motion underlying the measured electric signals. Since PERS can be interpreted on the basis of intramolecular charge displacements (15,29,30), we calculated the displacement of positive and negative charge centers—or, in other words, the change of the electric dipole moment vector of the bacteriorhodopsin molecule—between the ground state and the L intermediate of all three crystallographic structures. Unlike in Dér et al. (14), we considered only the z component of the difference dipole vector ($\mu^{z}_{\mathrm{bR-L}}$), since our measurements were restricted to the detection of charge displacements in the direction of the membrane normal. Bearing in mind that the μ-values may depend sensitively on partial charges (PC), we calculated them according to two different sets of PC (27,28) (Table 1, *column 7*). Having the z axis of the x-ray structures pointing opposite to the overall pumping direction (Fig. 5), 1UCQ yields a positive value, whereas 1O0A and 1E0L give a smaller and a larger negative value, respectively, for the resulting charge displacement at both PC sets. Further analyzing the data of this calculation (Table 1, *columns 1–6*), we can establish that in all three models, besides the retinal moiety, only the charged amino acid side chains make a considerable contribution to $\mu^{z}_{\mathrm{bR-L}}$. It is also apparent that data calculated from 1UCQ and 1E0P show an overall similarity in terms of $\Delta\mu$-values of particular side chains, and the main difference comes from the motion of Arg-82 in the latter. In 1O0A, Arg-82 shifts to the opposite direction, and the contribution from turnover of the Schiff-base proton is missing.

Another important contribution to the resulting charge displacement is assumed to come from water molecules. Since the dipole moment of freely rotating water molecules is smeared out, they do not contribute to the electric signals, nor does the migration of water molecules itself. However, those ''bound'' water molecules that change their orientation

TABLE 1 The *z* component of the electric dipole moment change between bR and L (μ^z_{bR-L}) calculated from three crystallographic L structures

L structure	Arg-82	Asp-85	Leu-93	Trp-182	Asp-212	Lys-216	Prot	Prot + water
1E0P	−2.1734	0.1631	0.0125	0.1189	0.2184	0.5451	−1.1154	−0.3404
	−1.8833	0.1532	0.0174	0.0602	0.2025	0.6250	−0.8250	−0.0500
1O0A	0.6143	−0.2344	−0.0171	−0.0059	−0.1918	−0.2212	−0.0560	0.7190
	0.6145	−0.2395	−0.0154	−0.0001	−0.2299	−0.3889	−0.2593	0.5157
1UCQ	0.2224	0.0608	−0.0061	0.0486	−0.2201	0.2448	0.3504	1.1254
	0.2078	0.0704	−0.0056	0.0314	−0.2422	0.2319	0.2937	1.0687

The contribution of the considered amino acid side chains and the retinal (included in Lys-216), and their sum without (Prot) and with (Prot + water) the assumed contribution of a water molecule (31) is listed. Dipole changes, all given in eÅ units, are calculated from two partial-charge-value data sets (27,28).

during the bR-L transition are expected to affect the overall dipole change. Each of the three L structures contains three water molecules in the vicinity of retinal, but x-ray experiments do not carry direct information on their orientation. There is Fourier transform infrared evidence, however, in favor of a flip-flop motion of a water molecule during the K→L transition (31). Since the dipole of this water molecule is assumed to be quasiparallel with our *z* axis, its turnover would give a contribution of some 0.775 eÅ to the resulting dipole values (Table 1, *column 8*).

From our experiments, it follows that both components of the electric signal associated with the bR→L transition reflect dipole changes corresponding to the displacement of a positive charge opposite to the overall pumping direction.

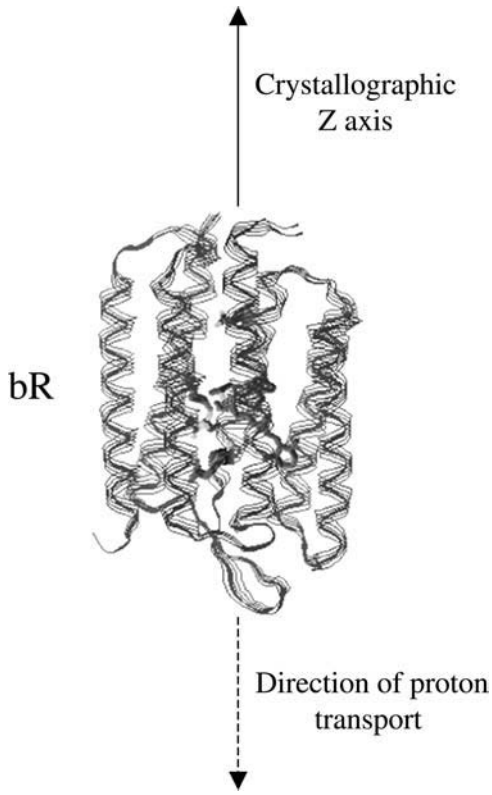

FIGURE 5 Demonstration of the crystallographic *z* axis and the direction of proton transport with respect to the bR molecule.

This implies that, in the coordinate system used for the x-ray data, μ^z_{bR-L} must be positive (Fig. 5). The absolute value of the dipole change associated with the bR-L transition can also be estimated, if we consider that the time integral of the full electric signal (integrated through the time course of the whole photocycle) should correspond to a full displacement of a proton through the membrane, i.e., to a 45 eÅ dipole change. Taking this value as a reference, on the basis of our measurements we can estimate μ^z_{bR-L} to be some 1.3 eÅ. Comparing this value with the data of Table 1, column 8, we can see that the data from 1UCQ best approach this value (~1.1 eÅ). However, to tell anything more definite, further molecular dynamics calculations starting from the x-ray structures are necessary (32–34) to establish the exact effect of water molecules and the retinal polarization (35) on the overall charge displacement.

In general, we can establish that comparison of dipole change values determined from both time-resolved measurements of electric signals and x-ray structures gives valuable results. On the one hand, intramolecular charge rearrangements, as the main contributors to the electric signals associated with the photocycle, can be identified, and on the other hand, PERS is suggested to be used as a sensitive experimental test for the verification of intermediate structures. The results also call attention to a general need of improving refinement procedures of raw x-ray data (e.g., by more extensive molecular dynamics calculations), so as to better approach native protein structures.

SUPPLEMENTARY MATERIAL

An online supplement to this article can be found by visiting BJ Online at http://www.biophysj.org.

The authors are grateful to Prof. Klaus Schulten and to Drs. William Humphrey and László Fábián for their kind help in providing the partial charge sets. Financial support from the Hungarian National Science Fund OTKA T-049489 is very gratefully acknowledged.

REFERENCES

1. Lanyi, J. K. 1997. Mechanism of ion transport across membranes. Bacteriorhodopsin as a prototype for proton pump. *J. Biol. Chem.* 272: 31209–31212.

2. Stoeckenius, W. 1999. Bacterial rhodopsins: evolution of a mechanistic model for the ion pump. *Protein Sci.* 8:447–459.
3. Lanyi, J. K. 2000. Bacteriorhodopsin. *Biochim. Biophys. Acta.* 1640:1–3.
4. Balashov, S. P. 1995. Photoreactions of the photointermediates of bacteriorhodopsin. *Isr. J. Chem.* 35:415–428.
5. Lanyi, J. K. 2004. X-ray diffraction of bacteriorhodopsin photocycle intermediates. *Mol. Membr. Biol.* 21:143–150.
6. Lanyi, J. K. 2004. Bacteriorhodopsin. *Annu. Rev. Physiol.* 66:665–688.
7. Luecke, H., and J. K. Lanyi. 2003. Structural clues to the mechanism of ion pumping in bacteriorhodopsin. *Adv. Protein Chem.* 63:111–130.
8. Lanyi, J. K., and B. Schobert. 2003. Mechanism of proton transport in bacteriorhodopsin from crystallographic structure of the K, L, M_1, M_2 and M_2' intermediates of the photocycle. *J. Mol. Biol.* 328:439–450.
9. Luecke, H., B. Schobert, H. T. Richter, J. P. Cartailler, and J. K. Lanyi. 1999. Structural changes in bacteriorhodopsin during ion transport at 2 Å resolution. *Science.* 286:255–260.
10. Royant, A., K. Edman, T. Ursby, E. Pebay-Peyroula, E. M. Landau, and R. Neutze. 2000. Helix deformation is coupled to vectorial proton transport in the photocycle of bacteriorhodopsin. *Nature.* 406:645–648.
11. Kouyama, T., T. Nishikawa, T. Tokuhisa, and H. Okamura. 2004. Crystal structure of the L intermediate of bacteriorhodopsin: evidence for vertical translocation of a water molecule during the proton pumping cycle. *J. Mol. Biol.* 335:469–481.
12. Edman, K., A. Royant, G. Larsson, F. Jacobson, T. Taylor, D. van der Spoel, E. M. Landau, E. Pebay-Peyroula, and R. Neutze. 2004. Deformation of helic C in the low temperature L-intermediate of bacteriorhodopsin. *J. Biol. Chem.* 279:2147–2158.
13. Lanyi, J. K. 2004. What is the real crystallographic structure of the L photointermediate of bacteriorhodopsin? *Biochim. Biophys. Acta.* 1658: 14–22.
14. Dér, A., L. Oroszi, Á. Kulcsár, L. Zimányi, R. Tóth-Boconádi, L. Keszthelyi, W. Stoeckenius, and P. Ormos. 1999. Interpretation of the spatial charge displacements in bacteriorhodopsin in terms of structural changes during the photocycle. *Proc. Natl. Acad. Sci. USA.* 96:2776–2781.
15. Keszthelyi, L., and P. Ormos. 1980. Electric signals associated with the photocycle of bacteriorhodopsin. *FEBS Lett.* 109:189–193.
16. Karvaly, B., and Zs. Dancsházy. 1977. Photoreactions of the photointermediates of bacteriorhodopsin. *FEBS Lett.* 76:36–40.
17. Ormos, P., Zs. Dancsházy, and L. Keszthelyi. 1980. Electric response of a back photoreaction in the bacteriorhodopsin photocycle. *Biophys. J.* 31:207–213.
18. Ludmann, K., C. Ganea, and G. Váró. 1999. Back photoreaction from intermediate M of bacteriorhodopsin photocycle. *J. Photochem. Photobiol. B.* 49:23–28.
19. Dickopf, S., and M. P. Heyn. 1997. Evidence for the first phase of the reprotonation switch of bacteriorhodopsin from time-resolved photovoltage and flash photolysis experiments on the photoreaction of the M-intermediate. *Biophys. J.* 73:3171–3181.
20. Ormos, P., L. Reinisch, and L. Keszthelyi. 1982. Fast electric response signals in the bacteriorhodopsin photocycle. *Biochim. Biophys. Acta.* 732:471–479.
21. Trissl, H.-W., W. Gärtner, and W. Leibl. 1989. Reversed picosecond charge displacement from the photoproduct K of bacteriorhodopsin demonstrated photoelectrically. *Chem. Phys. Lett.* 158:515–518.
22. Groma, G. I., J. Hebling, C. Ludwig, and J. Kuhl. 1995. Charge displacement in bacteriorhodopsin during the forward and reverse bR-K phototransition. *Biophys. J.* 69:2060–2065.
23. Tóth-Boconádi, R., A. Szabó-Nagy, S. G. Taneva, and L. Keszthelyi. 1999. Photoelectric response of the N intermediate of bacteriorhodopsin and its mutant T46V. *FEBS Lett.* 499:5–8.
24. Tóth-Boconádi, R., L. Keszthelyi, and W. Stoeckenius. 2003. Photoexcitation of the O- intermediate in bacteriorhodopsin mutant L93A. *Biophys. J.* 84:3857–3863.
25. Tóth-Boconádi, R., S. G. Taneva, and L. Keszthelyi. 2001. Photoexcitation of the O intermediate of bacteriorhodopsin and its mutant E204Q. *J. Biol. Phys. Chem.* 1:58–63.
26. Dér, A., P. Hargittai, and J. Simon. 1985. Time resolved photoelectric and absorption signals from oriented purple membranes immobilized in gels. *J. Biochem. Biophys. Methods.* 10:295–300.
27. Humphrey, W., D. Xu, M. Sheves, and K. Schulten. 1995. Molecular dynamics study of the early intermediates in the bacteriorhodopsin photocycle. *J. Phys. Chem.* 99:14549–14560.
28. MacKerell, A. D., Jr., B. Brooks, C. L. Brooks III, L. Nilsson, B. Roux, Y. Won, and M. Karplus. 1998. CHARMM: the energy function and its parameterization with an overview of the program. *In* The Encyclopedia of Computational Chemistry. P. von Ragué Schleyer, editor. John Wiley & Sons, Chichester. 271–277.
29. Dér, A., and L. Keszthelyi. 2001. Charge motion during the photocycle of bacteriorhodopsin. *Biochemistry (Mosc.).* 66:1234–1248.
30. Oroszi, L., A. Dér, and P. Ormos. 2002. Theory of electric signals of membrane proteins in three dimensions. *Eur. Biophys. J.* 31:136–144.
31. Kandori, H. 2004. Hydration switch model for the proton transfer in the Schiff base region of bacteriorhodosin. *Biochim. Biophys. Acta.* 1658: 72–79.
32. Bondar, A.-N., F. Fischer, J. C. Smith, M. Elstner, and S. Suhai. 2004. Key role of electrostatic interaction in bacteriorhodopsin proton transfer. *J. Am. Chem. Soc.* 126:14668–14677.
33. Bondar, A.-N., M. Elstner, S. Suhai, J. C. Smith, and S. Fischer. 2004. Mechanism of primary proton transfer in bacteriorhodosin. *Structure.* 12:1281–1288.
34. Bondar, A.-N., S. Fischer, S. Suhai, and J. C. Smith. 2005. Tuning of retinal twisting in bacteriorhodopsin controls the directionality of the early photocycle steps. *J. Phys. Chem. B.* 109:14786–14788.
35. Tajkhorshid, E., B. Paizs, and S. Suhai. 1999. Role of isomerization barriers in the pK(a) control of the retinal Schiff base: a density functional study. *J. Phys. Chem. B.* 103:4518–4527.